

Quasicrystalline Structure of Icosahedral $\text{Al}_{68}\text{Pd}_{23}\text{Mn}_9$ Resolved by Scanning Tunneling Microscopy

Thomas M. Schaub, Daniel E. Bürgler, and H.-J. Güntherodt
Institut für Physik, Universität Basel, Klingelbergstrasse 82, CH-4056 Basel, Switzerland

J. B. Suck
Institut Laue-Langevin, BP156, F-38042 Grenoble Cedex 9, France
 (Received 28 April 1994)

For the first time the surface structure of an icosahedral quasicrystal could be resolved in direct space by scanning tunneling microscopy. The surface was found to form terraces with their normals being parallel to a fivefold axis. On the terraces fivefold stars and pentagonal holes were observed. Both the step heights and the distances between pentagonal holes obey Fibonacci sequences. The distribution of the holes locally resembles a Penrose tiling and is correlated up to long distances indicating a quasiperiodic order. A simple model yields an autocorrelation function very similar to the experiment.

PACS numbers: 61.44.+p, 68.35.Bs

Since the discovery of the first quasicrystal by Shechtman and co-workers [1], a considerable amount of experimental and theoretical work has been done in order to understand the complicated atomic structure of quasiperiodic lattices. Most of the experimental effort is based on x-ray and neutron diffraction investigating the reciprocal space of quasicrystals. Microscopic methods with high resolution as transmission electron microscopy (TEM) and scanning tunneling microscopy (STM) [2] were successfully applied to image decagonal phases [3–5], i.e., two-dimensional quasicrystals with crystalline periodicity along a tenfold screw axis. However, these high resolution methods have been applied to three-dimensional quasicrystals with less success [6–8]. In this Letter we present the first successful investigation of a three-dimensional icosahedral quasicrystal by STM.

For our investigations we chose the thermodynamically stable icosahedral phase of the ternary AlPdMn system [9,10], the atomic structure of which was already investigated using scattering methods [11]. A cm-size ingot of the approximate average chemical composition $\text{Al}_{68}\text{Pd}_{23}\text{Mn}_9$ was produced by Bridgman technique in an Al_2O_3 crucible. The ingot consisted of several mm-size quasicrystalline monograins. A disk of about 8 mm diameter was cut from the ingot perpendicularly to the growth direction. As the ingot mainly grew along a twofold axis [12], the surface normal of our sample should be approximately parallel to a twofold axis of most of the monograins. The sample was mechanically polished using standard methods. Upon heating the sample to about 700 K in vacuum, some material of unknown chemical composition segregated to the surface. However, after a few cycles of polishing and heating, this segregation terminated. Subsequently, the sample was cleaned in ultra-high vacuum (UHV) by cycles of ion-sputtering (1 keV Ar^+) and annealing at temperatures of up to 1050 K,

until no traces of oxygen or other impurities could be detected by *in situ* x-ray photoelectron spectroscopy. Finally, some of the monograins showed a sharp fivefold LEED (low energy electron diffraction) pattern dominated by rings each consisting of ten spots. As the sample surface became markedly rough by the treatment in UHV, microfacets orientated perpendicularly to a fivefold axis apparently formed as has been already observed experimentally [13] and suggested by theory [14] and Monte Carlo simulations [15].

STM investigations were performed by a home-built UHV instrument operating at a base pressure of 10^{-11} mbar. All images presented here were measured in the constant current mode with the sample being at positive bias voltage. We used an electrochemically etched W tip.

STM images of the clean surface show atomically flat terraces (Fig. 1) [16], which seem to be similar to the terraces of ordinary periodic crystals. However, further inspection of the step heights appearing in this image yields two incommensurable values: $H = 6.78 \pm 0.24 \text{ \AA}$ for the higher and $L = 4.22 \pm 0.26 \text{ \AA}$ for the lower step height, giving a ratio of 1.61 ± 0.12 , very close to the “golden mean” $\tau = (1 + \sqrt{5})/2 \approx 1.618$. The flat terraces visible in Fig. 1 are separated by steps, which form the following sequence: *HHLHHLHLHH*. This is actually part of the Fibonacci sequence, *LHHLHHLHLHLHLH* ..., which can be found iteratively. From theoretical considerations [17] one indeed expects an icosahedral quasicrystal to be faceted at the surface exhibiting rather flat faces (“terraces”) perpendicular to a fivefold axis of the quasicrystal. Only two different step heights should occur obeying part of the Fibonacci sequence, and the ratio of the higher and lower step height should be τ . We now have to show that the surface normals of the terraces in 1 are parallel to a fivefold axis in order to confirm the predictions of

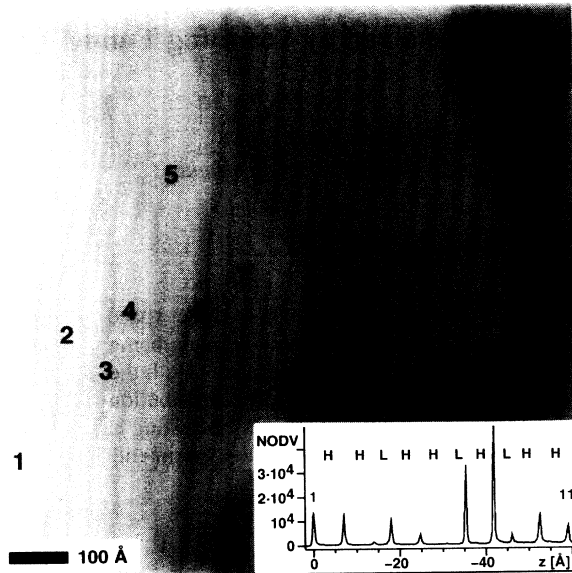


FIG. 1. Surface area of icosahedral $\text{Al}_{68}\text{Pd}_{23}\text{Mn}_9$ with atomically flat faces similar to terraces on an ordinary periodic crystal. The size of the STM image is $1000 \times 1000 \text{ \AA}^2$. For a better visualization of the stepped surface structure we added the x derivative to the plane-subtracted raw data. The inclination of the subtracted plane is $\approx 14^\circ$ ($U_{\text{bias}} = +1.93 \text{ V}$, $I_{\text{tunnel}} = 4.7 \text{ pA}$). Inset: The histogram of data values taken from the raw data describes the absolute frequency of measured z values (NODV: number of data values) and shows that two different step heights H and L appear. They occur in the sequence $HHLHHLHHLH$, which is part of the Fibonacci sequence.

[17]. From LEED measurements we only know about the existence of ordered surface areas with fivefold symmetry. High resolution STM images allow us to conclude that the atomic structure on the terraces in Fig. 1 are indeed responsible for the fivefold-symmetric LEED pattern. Figure 2 presents an STM image of a large terrace (number 8 of Fig. 1). Some objects of clearly fivefold symmetry immediately attract attention: fivefold stars aligned to each other (view along the white arrow in Fig. 2) and small holes of pentagonal shape, often surrounded by five atomic-sized protrusions of $\approx 4 \text{ \AA}$ diameter (see inset of Fig. 2) that possibly are single atoms. These pentagonal holes are found to have the same size and orientation all over the terrace. Five of them often create a larger pentagon (e.g., near the right hand side of the arrow in Fig. 2), a structure that is self-similar to the pentagonal holes. Sometimes almost complete decagonal rings are formed by the holes resembling the arrangement of Penrose tiles [18]. Therefore we assume that the distribution of the pentagonal holes reflects the quasicrystalline nature of the sample and tentatively draw a line grid parallel to the five edges of the holes, which at the same time are the "bond directions" between the atomic-sized protrusions surrounding the holes. In Fig. 2 only one set of parallel lines out of five is

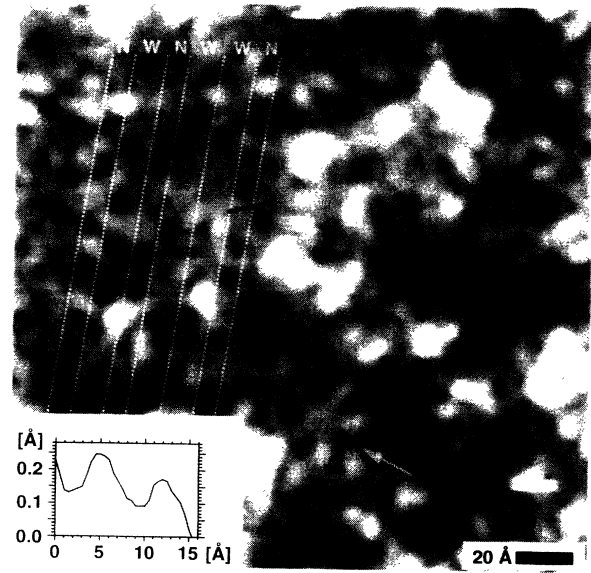


FIG. 2. $200 \times 200 \text{ \AA}^2$ -sized high resolution STM image showing surface details with fivefold symmetry. When viewing along the white arrow at least three fivefold stars aligned with each other are visible. A set of grid lines (dotted) running in one direction of the edges of characteristic pentagonal holes is shown for illustration. Note the nonperiodic occurrence of two different line separations (W and N , see text). The pentagonal holes are often surrounded by five atomic-sized protrusions. A line section across two of them (black bar) is shown as inset. The image has been median-filtered to remove high frequent noise ($U_{\text{bias}} = +2.24 \text{ V}$, $I_{\text{tunnel}} = 43 \text{ pA}$, average corrugation on undisturbed regions: $\approx 0.5 \text{ \AA}$).

shown for clarity. The edges of most holes are perfectly aligned with respect to these lines. There are two incommensurable separations W (wide) and N (narrow), again forming part of the Fibonacci sequence as in the case of the step heights. Analyzing the lines drawn in Fig. 2 yields the values $W = 11.81 \pm 0.39 \text{ \AA}$ for the wider and $N = 7.38 \pm 0.38 \text{ \AA}$ for the narrower separation. Their measured ratio W/N of 1.60 ± 0.10 is close to τ . If one actually assumes τ to be the correct value, the values of W and N can be determined with higher accuracy. The total width of m wide and n narrow distances should be equal to $(m\tau + n)N$. Applying this method to analyze the overall pentagrid of the STM image shown in Fig. 2 one obtains $N = 7.17 \pm 0.08 \text{ \AA}$ and $\tau N = W = 11.60 \pm 0.13 \text{ \AA}$.

Comparing the results of our STM investigation to the structure model proposed by diffraction experiments [11] we find in Table I of [11] distances of 4.08 and 6.60 \AA between dense atomic planes perpendicular to a fivefold axis containing all three chemical species, which agree with our measured step heights L and H . We can also determine separations between rows of atoms of about 7.4 and 12 \AA within these planes (see Fig. 10 of [11]), which reasonably compare to our line separations N and W describing the distribution of pentagonal holes.

As some of the pentagonal holes do not fit to the pentagrid drawn into the STM image of Fig. 2, a two-dimensional correlation function of the holes, was calculated to shed light on the actual degree of quasiperiodic order. This was carried out by using a digitalization algorithm that extracts the pattern of holes from the image in Fig. 2 by assigning the value 1 to those parts of the image with data values smaller than a certain limit and 0 to the others. Then the autocorrelation function $A(\vec{r})$ of the "hole-image" $z_h(\vec{r})$, $\vec{r} = (x, y)$,

$$A(\vec{r}) = \int_{\mathcal{F}} z_h(\vec{r}') z_h(\vec{r} + \vec{r}') d^2 r',$$

was calculated numerically (see Fig. 3).

Surprisingly the holes are highly correlated: $A(\vec{r})$ clearly shows tenfold and fivefold symmetries and strong correlations up to long distances indicating a nearly perfect quasiperiodic order of our sample.

Now we will show that the distribution of the holes can be approximately described by an Ammann line grid by comparing $A(\vec{r})$ to a correlation function obtained from a suitable model. This model provides a reasonably similar autocorrelation function justifying our choice of the line grid that was matched to the holes of Fig. 2. Starting from a regular pentagon, groups of lines parallel to the five edges of the pentagon are drawn. The separations of the lines follow Fibonacci sequences with the ratio of the long to the short distance equal to τ (Ammann grid) and the short distance being the height of the initial pentagon.

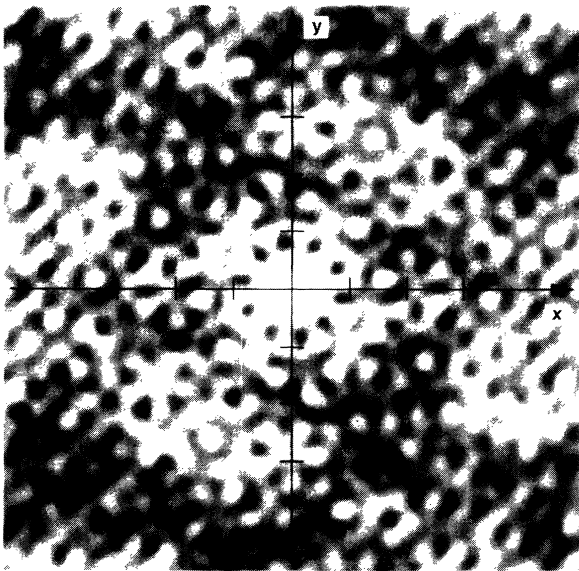


FIG. 3. Autocorrelation function $A(\vec{r})$ of the hole pattern extracted from Fig. 2. The center of the image corresponds to a displacement of $\vec{r} = (0,0)$. $A(\vec{r})$ extends to displacements of $\pm 100 \text{ \AA}$ in the x and y directions. The spacing between bars on the overlaid axes is 20 \AA . Correlation maxima appear as white spots in this image. Note the high correlation up to the edges of the image and the very clear fivefold symmetry.

If we select all pentagons of a certain size and orientation, which yield a hole density comparable to the experimental data, a pattern as depicted in the inset of Fig. 4 is obtained. The autocorrelation function of this pattern is given in Fig. 4: it strongly resembles the autocorrelation of the observed hole distribution exhibiting the same symmetry and long range order. By assigning the value $N = 7.17 \text{ \AA}$ to the height of the filled pentagons in the model grid, the calculated autocorrelation pattern can also be quantitatively compared to the measured one. Table I lists the radii $|\vec{r}|$ of the first ten correlation maxima (labelled I,II, ..., X in Fig. 4). For the first few maxima the agreement of the experimentally obtained and the calculated values is excellent. However, at larger radii the model predicts a few percent higher values than observed. This might indicate some relaxation of the quasicrystalline order at the surface towards higher density. A relaxation of a perfect icosahedral quasiperiodic lattice was also observed in computer simulations of quasicrystals based on realistic pair potentials [19,20].

In conclusion, we have investigated the surface of icosahedral $\text{Al}_{68}\text{Pd}_{23}\text{Mn}_9$ by STM. We found atomically flat terraces separated by steps of two different heights, the succession of these steps corresponds to a Fibonacci sequence. The lateral symmetry within the terraces was

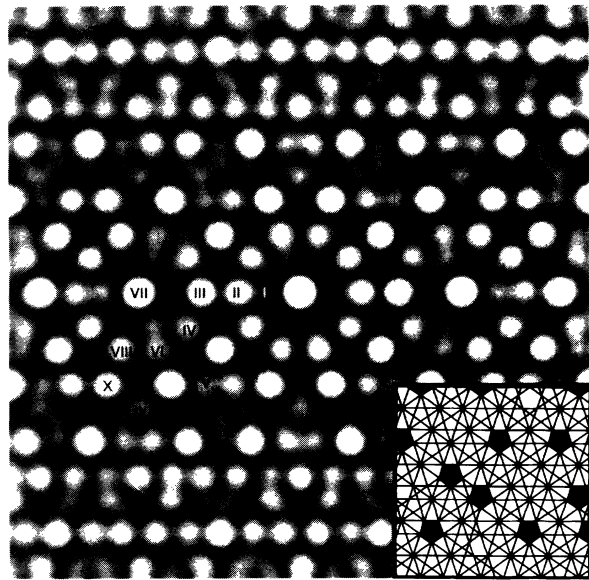


FIG. 4. Model autocorrelation function. All pentagons of a certain size and orientation were selected from an Ammann-type pentagrid, a part of which is shown in the inset. The calculated autocorrelation $A(\vec{r})$ of the black pentagons is shown using the same scale as for the inset. Deviations from exact fivefold or tenfold symmetry are due to the finite size of the model grid. The ten first correlation maxima are marked by Roman numerals for a better comparison to the experimental data (see Table I). After scaling the image suitably (see text) its size has been chosen to give about the same absolute displacements as in Fig. 3.

TABLE I. Radii of the correlation maxima in Fig. 3 (r_{exp}) and Fig. 4 (r_{calc}). The r_{calc} values were determined by identifying the height of the pentagons in the model grid (see inset of Fig. 4) with $N = 7.17 \text{ \AA}$. The estimated absolute error of all values is $\pm 0.3 \text{ \AA}$.

	I	II	III	IV	V	VI	VII	VIII	IX	X
$r_{\text{exp}} (\text{\AA})$	≈ 12	19.7	31.7	36.9	41.3	49.4	51.0	60.5	63.3	68.1
$r_{\text{calc}} (\text{\AA})$	12.1	19.8	31.9	37.3	43.3	50.1	51.8	60.9	64.6	69.7

determined to be fivefold. A line grid, which follows Fibonacci sequences, was matched to pentagonal holes on one of the terraces. The autocorrelation function of the holes shows the quasicrystalline order to be rather perfect and to extend to long distances. A simple model, which is based on an Ammann grid, reproduces orientation, distribution, and spatial correlation of the holes. Our observation of Fibonacci sequences vertically as well as laterally directly proves the three-dimensional quasiperiodic order of our sample at the atomic scale.

We are indebted to M. Audier, M. de Boissieu, M. Boudard, and H. Klein, who provided us with the AlPdMn monograins produced in the framework of the French GDR 5 program. The present study would not have been possible without their samples. We thank H.-U. Nissen and R. Schilling for valuable discussions. Financial support from the Swiss National Science Foundation and the Swiss *Kommission zur Förderung der wissenschaftlichen Forschung* is gratefully acknowledged.

- [1] D. Shechtman, I. Blech, D. Gratias, and J. W. Cahn, *Phys. Rev. Lett.* **53**, 1951 (1984).
- [2] Another promising method to image quasicrystals in real space has been introduced recently by M. Erbudak, H.-U. Nissen, E. Wetli, M. Hochstrasser, and S. Ritsch, *Phys. Rev. Lett.* **72**, 3037 (1994).
- [3] A. R. Kortan, R. S. Becker, F. A. Thiel, and H. S. Chen, *Phys. Rev. Lett.* **64**, 200 (1990).
- [4] H. Chen, S. E. Burkov, Y. He, S. J. Poon, and G. J. Shiflet, *Phys. Rev. Lett.* **65**, 72 (1990).
- [5] C. Beeli, H.-U. Nissen, and J. Robadey, *Philos. Mag. Lett.* **63**, 87 (1991).
- [6] R. S. Becker, A. R. Kortan, F. A. Thiel, and H. S. Chen,

- J. Vac. Sci. Technol. B* **9**, 867 (1991).
- [7] K. Hiraga, M. Hirabayashi, A. Inoue, and T. Masumoto, *Sci. Rep. Res. Inst. Tohoku Univ. Ser. A* **32**, 309 (1985).
- [8] M. de Boissieu, M. Durand-Charre, P. Bastie, A. Carabelli, M. Boudard, M. Bessiere, S. Lefebvre, C. Janot, and M. Audier, *Philos. Mag. Lett.* **65**, 147 (1992).
- [9] A. P. Tsai, A. Inoue, Y. Yokoyama, and T. Masumoto, *Mater. Trans. JIM* **31**, 98 (1990); *Philos. Mag. Lett.* **61**, 9 (1990).
- [10] Y. Yokoyama, A. P. Tsai, A. Inoue, and T. Masumoto, *Mater. Trans. JIM* **32**, 1089 (1991).
- [11] M. Boudard, M. de Boissieu, C. Janot, G. Heger, C. Beeli, H.-U. Nissen, H. Vincent, R. Ibberson, M. Audier, and J. M. Dubois, *J. Phys. Condens. Matter* **4**, 10 149 (1992).
- [12] M. Audier (private communication).
- [13] M. Audier, P. Guyot, and Y. Brechet, *Philos. Mag. Lett.* **61**, **55** (1990); C. Beeli and H.-U. Nissen, *Philos. Mag. B* **68**, 487 (1993).
- [14] J. Toner, *Phys. Rev. Lett.* **64**, 930 (1990).
- [15] J. A. Jaszczak, W. F. Saam, and B. Yang, *Phys. Rev. B* **39**, 9289 (1989); **41**, 6864 (1990).
- [16] Steps have recently been observed by atomic force microscopy on *i*-AlCuFe by K. Balzuweit and W. J. P. van Enkevort, *J. Cryst. Growth* **135**, 297 (1994).
- [17] C. L. Henley and R. Lipowsky, *Phys. Rev. Lett.* **59**, 1679 (1987); R. Lipowsky and C. L. Henley, *Phys. Rev. Lett.* **60**, 2394 (1988); A. Garg and D. Levine, *Phys. Rev. Lett.* **59**, 1683 (1987); A. Garg, *Phys. Rev. B* **37**, 10003 (1988); T. L. Ho, J. A. Jaszczak, Y. H. Li, and W. F. Saam, *Phys. Rev. Lett.* **59**, 1116 (1987).
- [18] R. Penrose, *Bull. Inst. Math. Appl.* **10**, 266 (1974).
- [19] T. Janssen, in *Quasicrystalline Materials*, edited by C. Janot and J. M. Dubois (World Scientific, Singapore, 1988), p. 327.
- [20] J. Hafner and M. Krajčič, *Europhys. Lett.* **13**, 335 (1990); *Phys. Rev. Lett.* **68**, 2321 (1992).

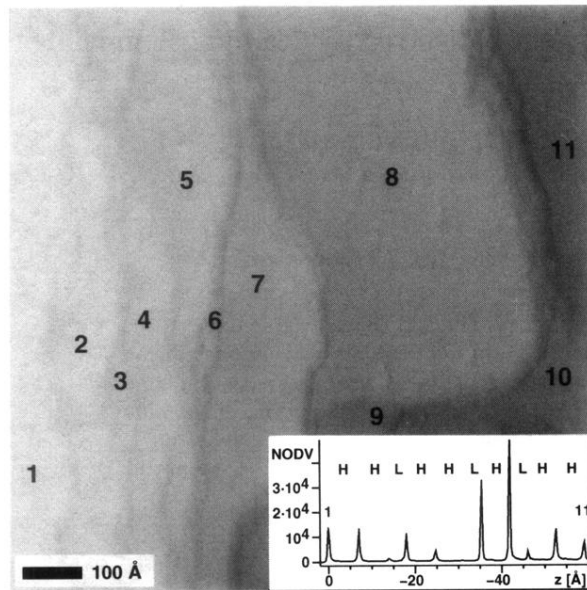


FIG. 1. Surface area of icosahedral $\text{Al}_{68}\text{Pd}_{23}\text{Mn}_9$ with atomically flat faces similar to terraces on an ordinary periodic crystal. The size of the STM image is $1000 \times 1000 \text{ \AA}^2$. For a better visualization of the stepped surface structure we added the x derivative to the plane-subtracted raw data. The inclination of the subtracted plane is $\approx 14^\circ$ ($U_{\text{bias}} = +1.93 \text{ V}$, $I_{\text{tunnel}} = 4.7 \text{ pA}$). Inset: The histogram of data values taken from the raw data describes the absolute frequency of measured z values (NODV: number of data values) and shows that two different step heights H and L appear. They occur in the sequence $HHLHLHLHH$, which is part of the Fibonacci sequence.

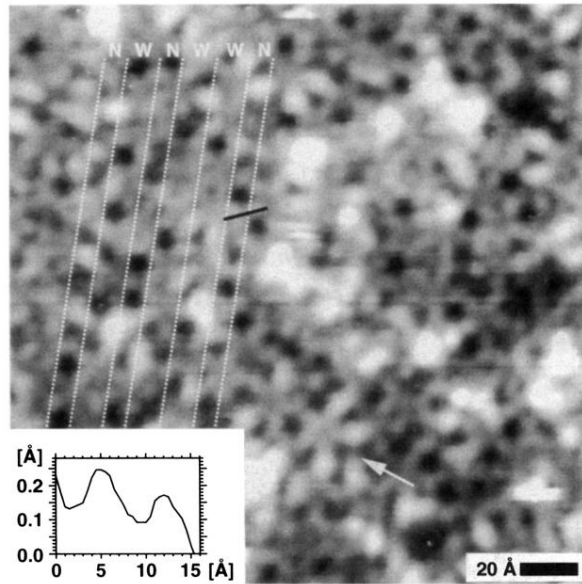


FIG. 2. $200 \times 200 \text{ \AA}^2$ -sized high resolution STM image showing surface details with fivefold symmetry. When viewing along the white arrow at least three fivefold stars aligned with each other are visible. A set of grid lines (dotted) running in one direction of the edges of characteristic pentagonal holes is shown for illustration. Note the nonperiodic occurrence of two different line separations (W and N , see text). The pentagonal holes are often surrounded by five atomic-sized protrusions. A line section across two of them (black bar) is shown as inset. The image has been median-filtered to remove high frequent noise ($U_{\text{bias}} = +2.24 \text{ V}$, $I_{\text{tunnel}} = 43 \text{ pA}$, average corrugation on undisturbed regions: $\approx 0.5 \text{ \AA}$).

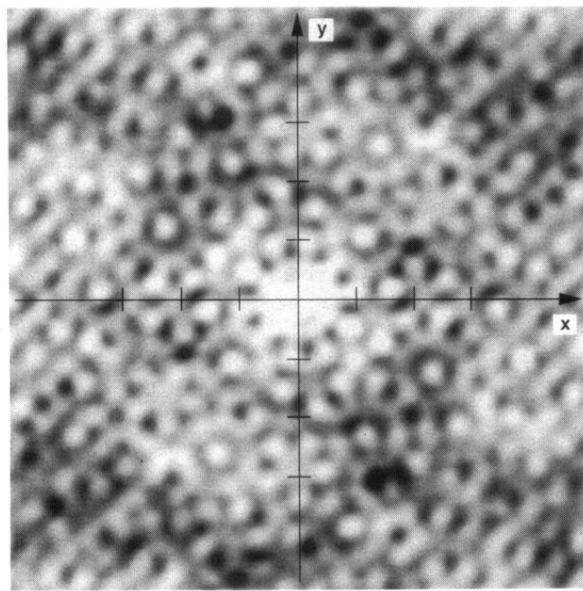


FIG. 3. Autocorrelation function $A(\vec{r})$ of the hole pattern extracted from Fig. 2. The center of the image corresponds to a displacement of $\vec{r} = (0,0)$. $A(\vec{r})$ extends to displacements of $\pm 100 \text{ \AA}$ in the x and y directions. The spacing between bars on the overlaid axes is 20 \AA . Correlation maxima appear as white spots in this image. Note the high correlation up to the edges of the image and the very clear fivefold symmetry.

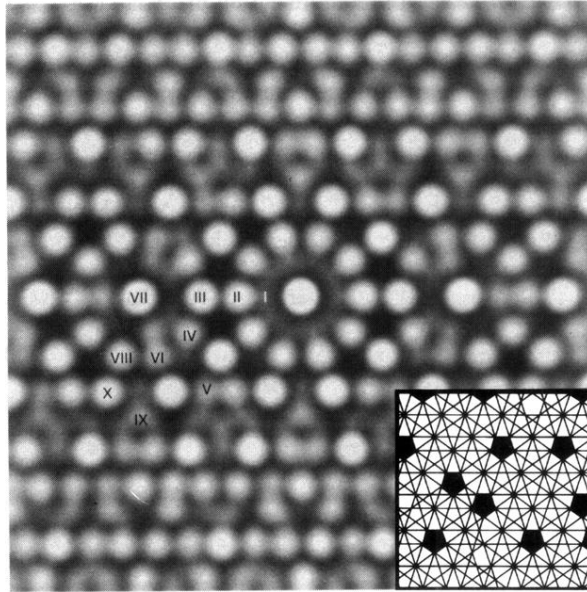


FIG. 4. Model autocorrelation function. All pentagons of a certain size and orientation were selected from an Ammann-type pentagrid, a part of which is shown in the inset. The calculated autocorrelation $A(\vec{r})$ of the black pentagons is shown using the same scale as for the inset. Deviations from exact fivefold or tenfold symmetry are due to the finite size of the model grid. The ten first correlation maxima are marked by Roman numerals for a better comparison to the experimental data (see Table I). After scaling the image suitably (see text) its size has been chosen to give about the same absolute displacements as in Fig. 3.